

Supporting Information

A Two-Photon AIEgen for Simultaneous Dual-Color Imaging of Atherosclerotic Plaques

Bo Situ^{a,b,†}, Meng Gao^{c,†}, Xiaojing He^{a,b,†}, Shiwu Li^e, Bairong He^{a,b}, Fengxia Guo^{a,b}, Chunmin Kang^{a,b}, Shan Liu^d, Lei Yang^d, Meijuan Jiang^{f,g}, Yanwei Hu^{a,b}, Ben Zhong Tang^{e,f,g,}, and Lei Zheng^{a,b,*}*

^aDepartment of Laboratory Medicine, Nanfang Hospital, Southern Medical University, Guangzhou, 510515, China.

^bGuangdong Engineering and Technology Research Center for Rapid Diagnostic Biosensors, Nanfang Hospital, Southern Medical University, Guangzhou 510515, China

^cNational Engineering Research Center for Tissue Restoration and Reconstruction, South China University of Technology, Guangzhou, 510006, China

^dDepartment of Pathology, Nanfang Hospital, Southern Medical University, Guangzhou, 510515, China

^eGuangdong Province Key laboratory of Biomedical Engineering, South China University of Technology, Guangzhou, 510006, China

^fDepartment of Chemistry and Hong Kong Branch of Chinese National Engineering Research Center for Tissue Restoration and Reconstruction, The Hong Kong University of Science & Technology, Clear Water Bay, Kowloon, Hong Kong, China

^gHKUST-Shenzhen Research Institute, No. 9 Yuexing 1st RD, South Area, Hi-tech Park, Nanshan, Shenzhen, 518057, China

[†] These authors contributed equally to this work.

Corresponding authors: nfyyzhenglei@smu.edu.cn (L.Z.), tangbenz@ust.hk (B.Z.T.)

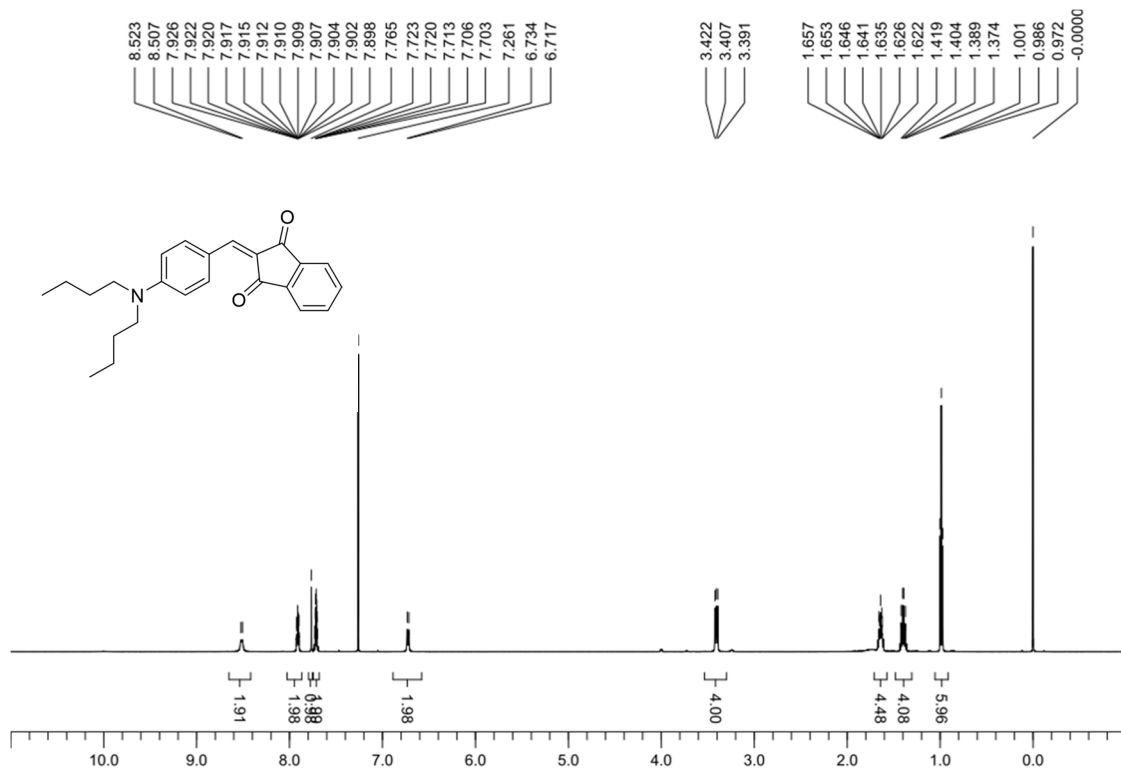


Figure S1. ¹H NMR spectra of IND (500 MHz, DMSO-*d*₆).

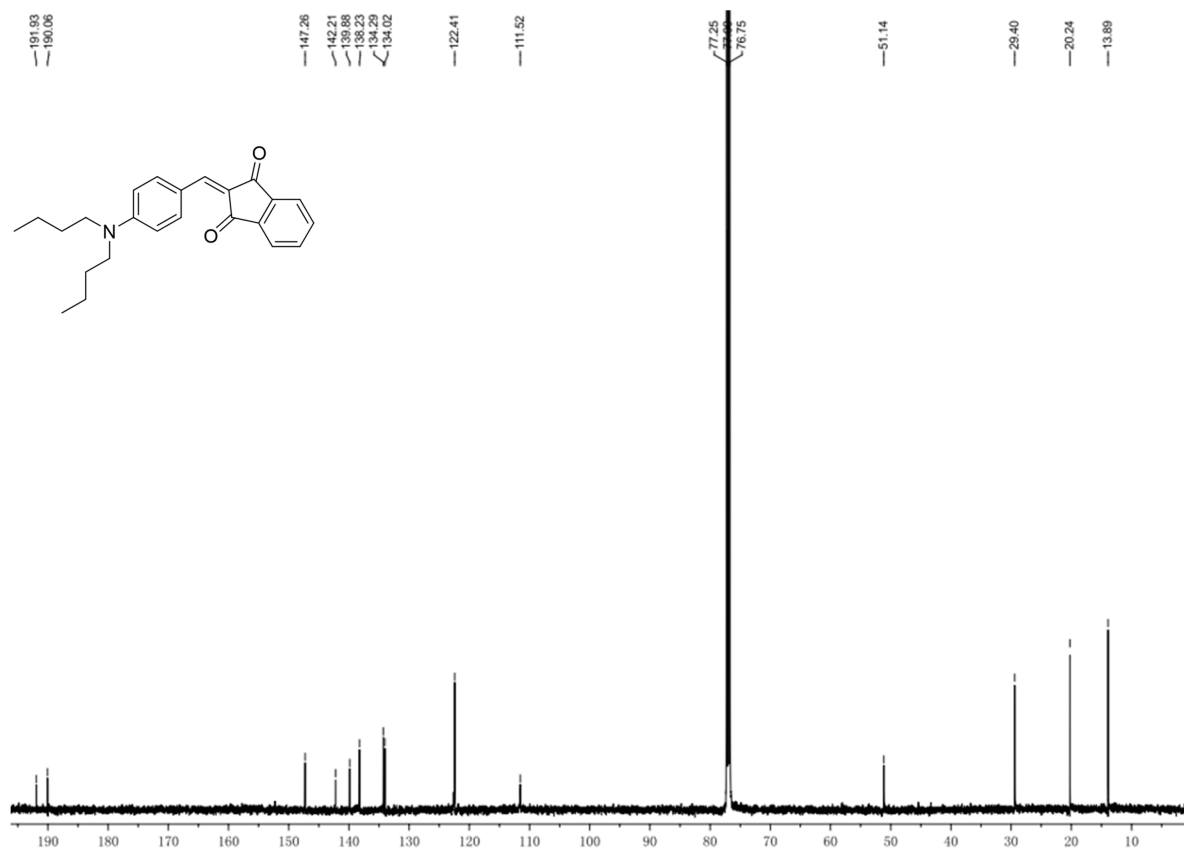


Figure S2. ¹³C NMR spectra of IND (125 MHz, DMSO-*d*₆).

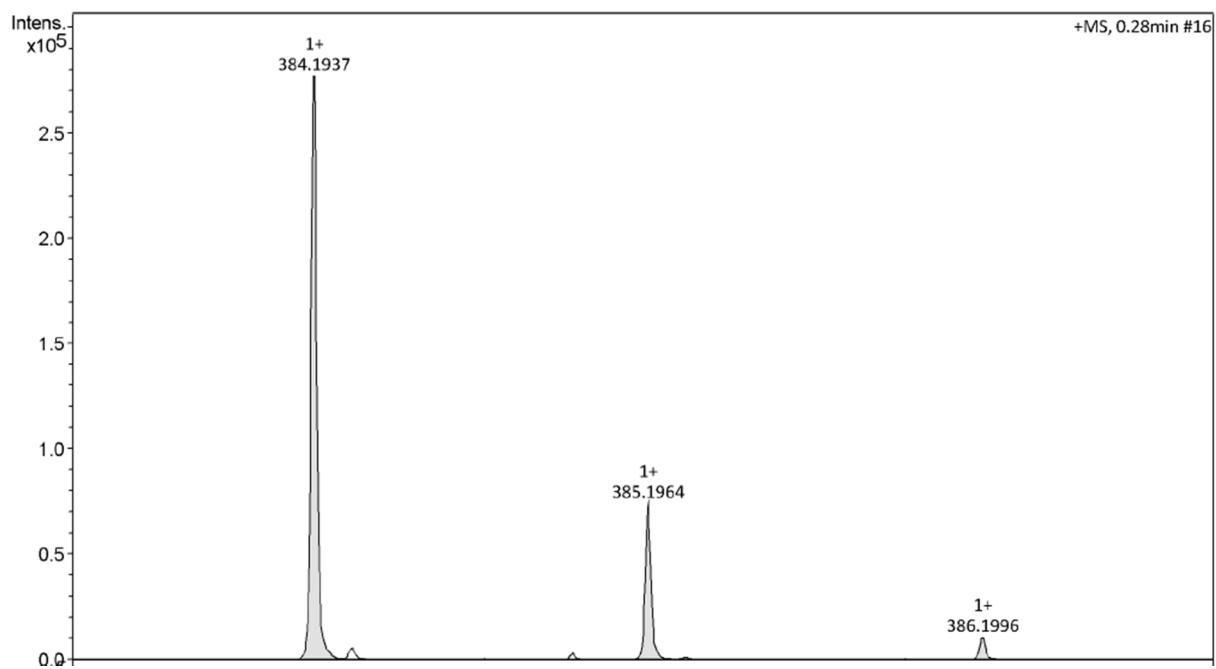


Figure S3. HRMS spectra of IND.

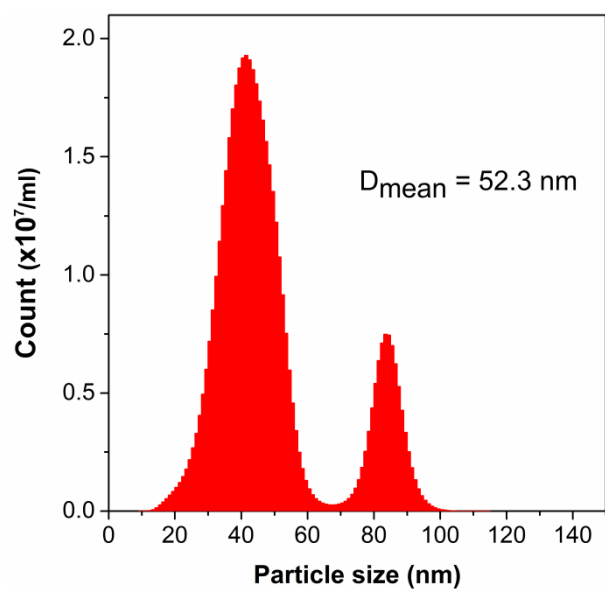


Figure S4. Particle size of aggregates of IND (10 μ M) formed in water.

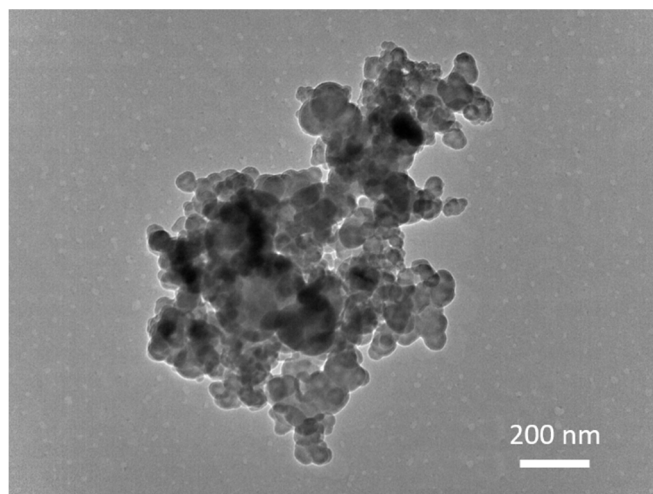


Figure S5. TEM image of IND aggregates.

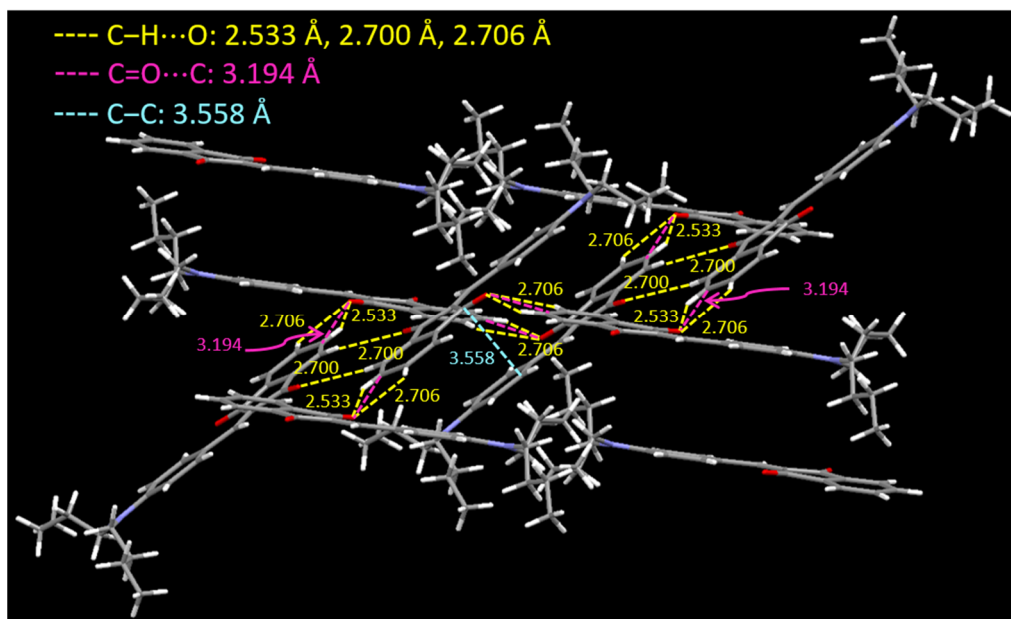


Figure S6. Multiple intermolecular interactions of IND in single crystal.

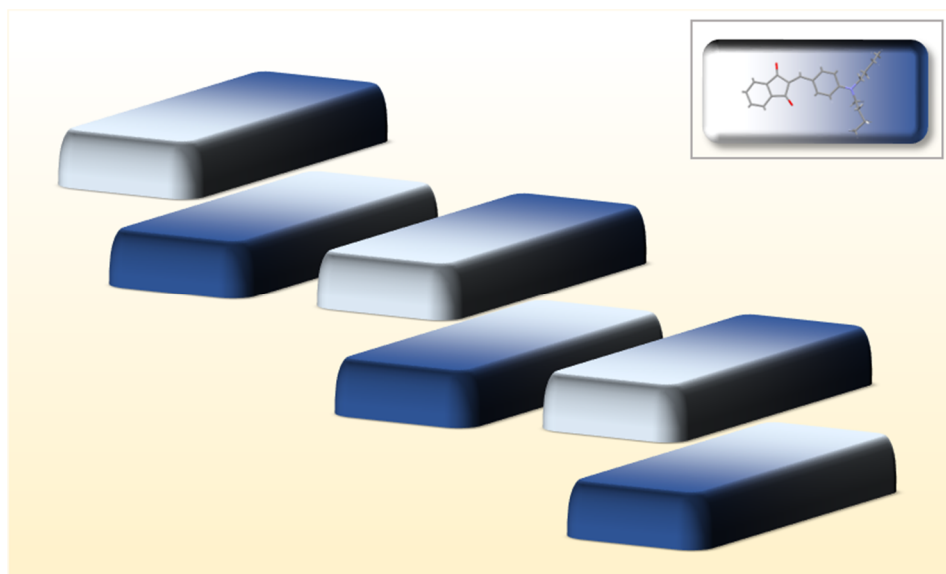


Figure S7. Representative diagram for the step-like packing mode of IND.

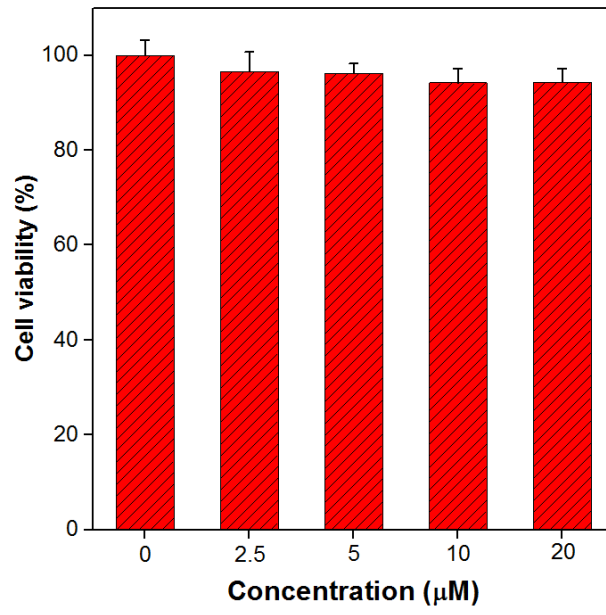


Figure S8. Cytotoxicity of IND on HeLa cells evaluated by a CCK-8 assay.

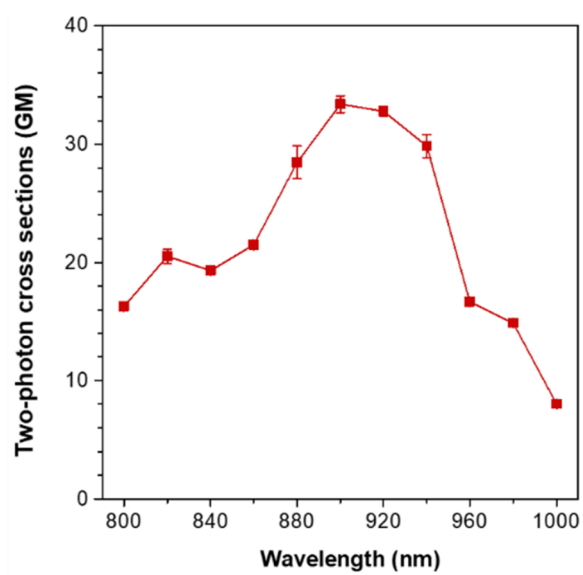


Figure S9. Two-photon absorption cross-sections of IND with fluorescein as the reference.

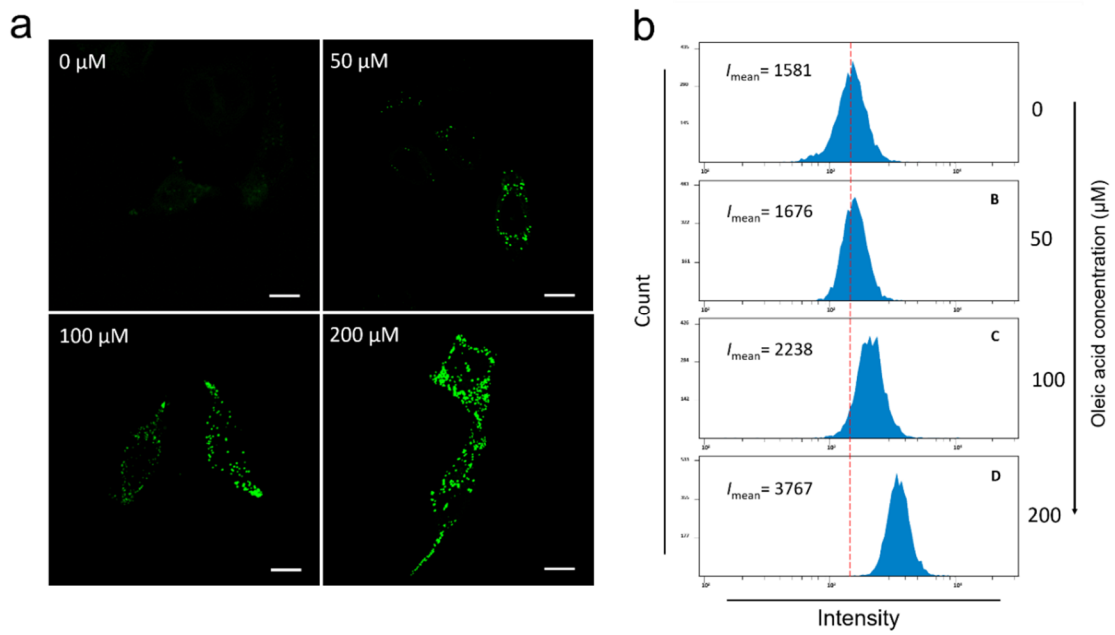


Figure S10. a) Representative two-photon fluorescence images of living HeLa cells stained with 20 μM IND for 30 minutes after treatment with different concentrations of oleic acid (0, 50, 100 and 200 μM). Quantitative measurement of the fluorescence of IND-labeled living HeLa cells after incubating with various concentrations of oleic acid by flow cytometry. $\lambda_{\text{ex}}=900$ nm for a) and $\lambda_{\text{ex}}=488$ nm for b). Scale bar, 15 μm.

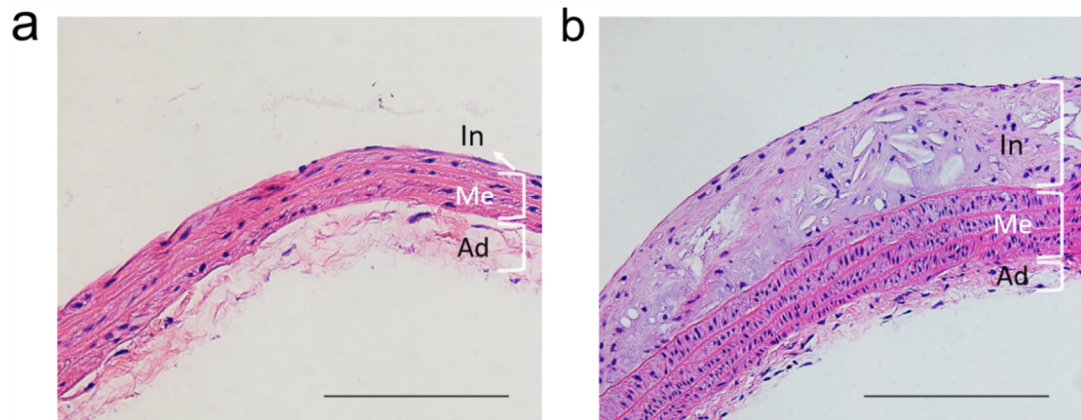


Figure S11. Histologic sectioned specimen of the mouse aorta stained with hematoxylin and eosin (H&E) indicating the intima (In), media (Me) and adventitia (Ad) in a) normal tissue and in b) atherosclerotic plaque of the artery. Scale bar, 200 μm .

Table S1. Photophysical properties of IND in THF/water mixture with different water fractions (f_w).

| f_w (%) | λ_{ab} [nm] ^{a)} | λ_{em} [nm] ^{b)} | Φ_F [%] ^{c)} | τ (ns) ^{d)} | k_r [10^7 S ⁻¹] ^{e)} | k_{nr} [10^8 S ⁻¹] ^{f)} |
|-----------|-----------------------------------|-----------------------------------|----------------------------|---------------------------|--|---|
| 0 | 484 | 528 | 0.6 | 0.97 | 0.62 | 10.25 |
| 80 | 509 | 549 | 0.3 | 1.79 | 0.17 | 5.57 |
| 99 | 493 | 632 | 9.8 | 5.43 | 1.80 | 1.66 |
| Solid | 515 | 637 | 11.7 | 11.1 | 1.05 | 0.80 |

a) Maximum absorption wavelength; b) Maximum emission wavelength; c) Absolute quantum yield; d) Average fluorescence lifetime; e) Radiative decay rate $k_r = \Phi/\tau$; f) Non-radiative decay rate $k_{nr} = (1-\Phi)/\tau$. [IND] = 10 μ M.

Additional supporting movies

Movie 1. Fluorescent change of sunflower oil after mixing with a same volume of water under 365 nm UV illumination. IND concentration, 10 μ M.

Movie 2. Representative 3D image of a living foam cell stained by IND under two-photon microscope excited by 900 nm laser.